

# WA98 Photon and CERES Dilepton Spectra: Spectral Red-Shift Versus Broadening

Jan-e Alam<sup>1,3</sup>, Pradip Roy<sup>2</sup>, Sourav Sarkar<sup>3</sup> and Bikash Sinha<sup>2,3</sup>

<sup>1</sup> *Physics Department, University of Tokyo, Tokyo 113-0033, Japan*

<sup>2</sup> *Saha Institute of Nuclear Physics, 1/AF Bidhannagar, Kolkata 700064*

<sup>3</sup> *Variable Energy Cyclotron Centre, 1/AF Bidhannagar, Kolkata 700064*

We estimate the photon and dilepton emission rates from hot hadronic matter with in-medium spectral shift and broadening of vector mesons. It is observed that both the WA98 photon data and CERES/NA45 dilepton data can be well reproduced with similar initial conditions. We argue that simultaneous measurement of the  $p_T$  spectra of single photons and invariant mass distribution of dileptons is important to understand the in-medium spectral function of the vector mesons.

PACS: 25.75.+r;12.40.Yx;21.65.+f;13.85.Qk

It is expected that the creation and study of quark gluon plasma (QGP) would be possible by effecting collisions of two nuclei at ultra-relativistic energies. Among various signals of QGP, photons and dileptons are known to be advantageous [1], because of their nature of interactions, those probe the entire volume of the plasma and thus, are better markers of the space time history of the matter formed after the collision. In this work we carry out a detailed analysis of the WA98 photon and CERES/NA45 dilepton data and emphasize that a simultaneous measurements of these is essential to understand the in-medium spectral function of vector mesons vis-a-vis red-shift and broadening.

We start with the single photon data of WA98 collaboration [2] which has initiated considerable theoretical activities [3-8]. For the analysis of WA98 photon spectra, we consider prompt photons resulting from the hard collisions of the partons in the colliding nuclei and the thermal photons from a hot hadronic gas with possible in-medium modifications. Photons from hadronic decays ( $\pi^0 \rightarrow \gamma\gamma$ ,  $\eta \rightarrow \gamma\gamma$  etc.) are already subtracted from the data [2] and hence we need not consider them here. We start our discussions with the prompt photon. The prompt photon yield for nucleus-nucleus collision is given by,

$$E \frac{dN}{d^3p} = n(b) \frac{1}{\sigma_{in}} E \frac{d\sigma_{pp}}{d^3p} \quad (1)$$

where  $n(b)$  is the average number of nucleon-nucleon collisions at an impact parameter  $b$ , and  $\sigma_{in}$  ( $=30$  mb, taken from Ref. [2]) is the  $p-p$  inelastic cross section. The average value of  $n(b)$  for collisions of two nuclei of mass numbers  $A$  and  $B$  is given by [9],

$$n(b) = AB T_{AB}(b) \sigma_{in} \quad (2)$$

where  $T_{AB}(b)$  is the nuclear overlap integral evaluated from the following expression,

$$T_{AB}(\vec{b}) = \int d^2s T_A(\vec{s}) T_B(\vec{b} - \vec{s}), \quad (3)$$

and the thickness function,  $T_A$  is defined as  $T_A(\vec{b}) = \int dz \rho_A(\vec{b}, z)$ . The nuclear density,  $\rho_A(\vec{b}, z)$  is parametrized by Wood-Saxon type profile function [10],

$$\rho_A(r) = \rho_0 \frac{1 + \omega r^2/R_A^2}{1 + e^{(r-R_A)/z}} \quad (4)$$

where  $\omega = 0$ ,  $z = 0.549$  for the Pb nucleus and  $R_A = 1.2A^{1/3}$  and the central density,  $\rho_0$  is determined by the normalization condition  $\int d^3r \rho_A(r) = 1$ . In Fig. 1  $n(b)$  is shown as a function of the impact parameter,  $b$ . The most central event in WA98 corresponds to  $b \sim 3.2$  fm/c. At this value of the impact parameter  $n(b) \sim 660$ . In the present analysis, we, therefore take this value of  $n(b)$  for the evaluation of prompt photon spectra.

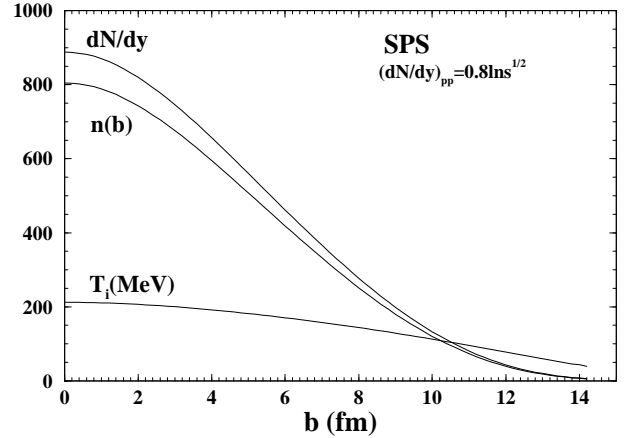


FIG. 1. Hadron multiplicity, effective number of nucleon-nucleon collisions and initial temperature as a function of impact parameter calculated by using Glauber model for nucleus - nucleus collisions (see text).

The prompt photon contributions has been evaluated with possible intrinsic transverse motion of the partons [4,11] inside the nucleon and multiplied by a  $K$ -factor  $\sim 2$ , to account for the higher order effects. The CTEQ(5M) parton distributions [12] have been used for evaluating hard photons. The relevant value of  $\sqrt{s}$ , energy in the centre of mass for WA98 experiment is 17.3

GeV. No experimental data on hard photons exist at this energy. Therefore, the “data” at  $\sqrt{s} = 17.3$  GeV is obtained from the data at  $\sqrt{s} = 19.4$  GeV of the E704 collaboration [13] by using the scaling relation,  $Ed\sigma/d^3p_\gamma |_{h_1+h_2 \rightarrow C+\gamma} = f(x_T = 2p_T/\sqrt{s})/s^2$ , for the hadronic process,  $h_1 + h_2 \rightarrow C + \gamma$  [14]. This scaling is valid in the naive parton model. However, such scaling may be spoiled in perturbative QCD due to the reasons, among others, the momentum dependence of the strong coupling,  $\alpha_s$  and from the scaling violation of structure functions, resulting in faster decrease of the cross section than  $1/s^2$  [11]. Therefore, the data at  $\sqrt{s} = 17.3$  GeV obtained by using the above scaling gives a conservative estimate of the prompt photon contributions. In the present work this has been used to reproduce the scaled  $p - p$  data. We have seen that the effects of the nuclear shadowing in parton distributions on the prompt photons are negligibly small at SPS but it is important at RHIC and LHC energies [15]. This is because the value of  $x(\sim 2p_T/\sqrt{s})$  at SPS is not small enough for the shadowing effects to be important.

It has been emphasized that the properties of hadrons will be modified due to its interaction with the particles in the thermal bath and such modifications will be reflected in the dilepton and photon spectra emitted from the system (see Refs. [16–20] for review). Broadly two types of medium modifications are expected: shift in the pole position and/or broadening of the spectral function.

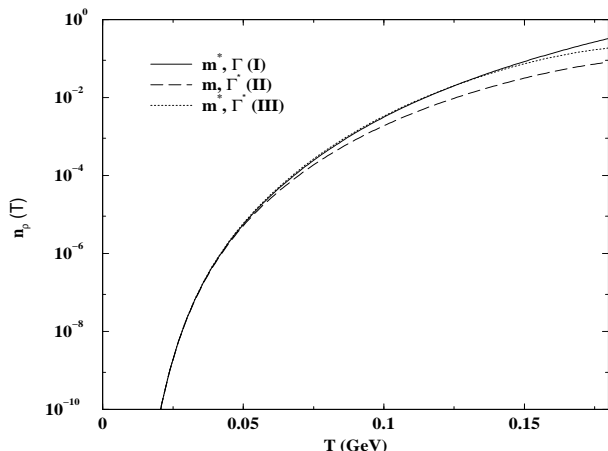


FIG. 2. Solid (long dashed) line represent density of thermal  $\rho$  as a function of temperature with in-medium mass and vacuum width (in-medium width and vacuum mass). Dotted line represents the density with medium mass and width.

We would like to see here whether the WA98 photon and CERES dilepton data can distinguish the following scenarios: (I) the system is formed in the hadronic phase with the hadronic masses (except pseudoscalars) approaching zero near the critical temperature according to the universal scaling law [16,21]

$$m_H^*/m_H = (1 - T^2/T_c^2)^{1/2} \quad (5)$$

but the width remains unchanged in the medium, (II)

the width of the vector meson ( $\rho$ ) increasing with temperature as,

$$\Gamma_\rho^* = \Gamma_\rho/(1 - T^2/T_c^2), \quad (6)$$

with their vacuum masses or the third scenario (III) both mass and width change according to eqs. 5 and 6 respectively. A fourth case, (IV) could be the one in which both the masses and width remain unchanged. In eqs. 5 and 6,  $T_c$  is the critical temperature (assumed as  $\sim T_i$  for simplicity) and the \* quantities denote the in-medium values of the hadronic masses ( $m_H^*$ ) and  $\rho$  decay width ( $\Gamma_\rho^*$ ). This study becomes important because the CERES dilepton data can not differentiate the above two scenarios (see the review [19]).

The photon production rates may be altered due to the in-medium modifications of thermal phase space factor as well as cross sections. The in-medium effects on the thermal phase space factor is demonstrated through  $\rho$  as it plays the most important role for the electromagnetic probes. In Fig. 2 we display the change in the density of thermal  $\rho$  as a function of temperature for scenarios (I), (II) and (III) by solid, long-dashed and dotted lines respectively. The density of  $\rho$  for both vacuum mass and width (scenario IV, not shown in the figure) does not show any appreciable difference from scenario II (long-dashed line). It is clear that the density of  $\rho$  is very sensitive to the spectral shift of  $\rho$  mass due to Boltzmann enhancement but rather insensitive to the change of width. The reason for small change in the density of  $\rho$  due to the in-medium broadening can be understood from the following arguments. The density of an unstable vector meson ( $\rho$  here) in a thermal bath can be written as [22],

$$\frac{dN}{d^3k d^3x ds} = \frac{g}{(2\pi)^3} \frac{1}{e^{\sqrt{k^2+s}/T} - 1} P(s) \quad (7)$$

where  $g$  is the statistical degeneracy of the particle and  $P(s)$  is the spectral function,

$$P(s) = \frac{1}{\pi} \frac{\text{Im} \Pi}{(s - m_\rho^2 - \text{Re} \Pi)^2 + (\text{Im} \Pi)^2} \quad (8)$$

$\text{Im} \Pi$  ( $\text{Re} \Pi$ ) is the imaginary (real) part of the  $\rho$  self energy. Eqs. 7 and 8 indicate that the density of particles (vector mesons) in a thermal bath is given by the Bose-Einstein distribution weighted by the Breit-Wigner function, which gets maximum weight from the point  $s = m_\rho^2 + \text{Re} \Pi$ , the contribution from either side of the maximum being averaged out. Therefore, the results become sensitive to the value of  $s = m_\rho^{2*} = m_\rho^2 + \text{Re} \Pi$  and not to the width of the spectral distribution. Note that  $P(s)$  tends to  $\delta(s - m_\rho^2 - \text{Re} \Pi)$  as  $\text{Im} \Pi \rightarrow 0$ , corresponding to a stable particle. (Here,  $\Pi$  is proportional to the trace of the self energy tensor  $\Pi_{\mu\nu}$  of the  $\rho$ ).

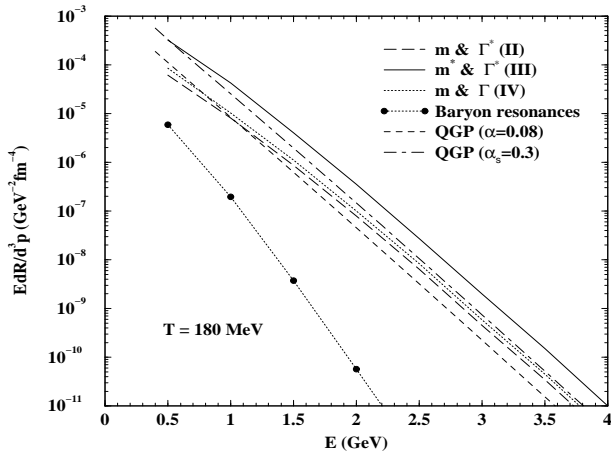


FIG. 3. The photon production rate as function of its energy at a temperature,  $T = 180$  MeV. Solid (long dashed) line indicates rate for scenario III (scenario II). Dotted line represents the spectra without any medium effects. Filled circles indicate photons originating from baryonic resonance decays. Short dashed (dot-dashed) line indicates the photon emission rate from a thermalized two-flavor quark gluon plasma for  $\alpha_s = 0.08(0.2)$ . Result for scenario I (not shown) does not differ from scenario III (the solid line).

To evaluate photon emission rate from hadronic matter we consider the processes [23,24]:  $\pi\rho \rightarrow \pi\gamma$ ,  $\pi\pi \rightarrow \rho\gamma$ ,  $\pi\pi \rightarrow \eta\gamma$ ,  $\pi\eta \rightarrow \pi\gamma$  and the decays  $\rho \rightarrow \pi\pi\gamma$  and  $\omega \rightarrow \pi\gamma$ . Photon production due to the process  $\pi\rho \rightarrow a_1 \rightarrow \pi\gamma$  [20] is also taken into consideration. In Fig. 3 the static (fixed temperature) photon spectra is shown for  $T = 180$  MeV. The solid line shows the enhanced yield with in-medium masses and decay widths compared to the yield obtained with vacuum masses and width (dotted line). The long-dashed line showing the result with in-medium width and vacuum masses does not differ substantially from the dotted line, because we find that the effects of the change in the decay width both on the phase space and the production cross section are small. We observe that the contributions from the decays of baryonic resonances ( $N(1520)$ ,  $N(1535)$ ,  $N(1440)$ ,  $\Delta(1232)$ , and  $\Delta(1620)$ ) are also small (filled circle). The values of the decay widths,  $R \rightarrow N\gamma$ , where  $R$  and  $N$  denote the baryonic resonances and the nucleon respectively, are taken from the particle data book. It is observed that the photon yield with universal mass variation scenarios, I and III is almost an order magnitude larger than the case II with large broadening of the  $\rho$ . The scenario (III) gives result similar to (I). Reduction in the hadronic masses causes an enhancement in the thermal distribution of mesons because of which the rate of thermal emission of photons increases. The scenario with vacuum values for both masses and width does not show any appreciable difference from (II). For the sake of comparison we have also shown the photon emission rate from a thermalized QGP. The photon spectra from QGP includes Compton, annihilation, bremsstrahlung and annihilation with scattering processes [23,25,26] (see also [27–29]). From

the lattice results [30] the value of  $\alpha_s \sim 0.3(g^2 = 4)$  at  $T = 180$  MeV. At  $T = 180$  MeV the emission rates from the QGP (dot-dashed) and hot hadronic matter (scenario II and IV) are comparable for  $p_T > 1.5$  GeV. The photon yield from hadronic matter for scenario I (and III) is substantially larger than that from QGP. However, it should be mentioned here that the photon emission rate from QGP is evaluated in Refs. [23,25,26] by using hard thermal loop (HTL) approximations, which is valid for the value of the color charge,  $g \ll 1$ . The validity of the HTL approximation to higher values of  $g$  is doubtful. In fact, such an extrapolation in the value of  $g$  (from  $g \ll 1$  to  $\sim 2$ ) introduces an uncertainty by a factor of  $\sim 5$ . Due to these uncertainties we must be careful in making any firm conclusion from the results obtained on the basis of the HTL approximations. For  $\alpha_s = 0.08(g = 1)$  the emission rate from QGP (short-dashed line) is much smaller than the rates from hadronic matter.

To compare the photon yield with experimental data we need to convolute the static (fixed temperature) rate with the space time evolution of the system - from the initial state to the freeze-out state. The value of the initial temperature is estimated as described below.

The hadron multiplicity in A + B collisions at an impact parameter  $b$  can be evaluated in terms of the multiplicity in  $pp$  collisions from the following expression [9],

$$\frac{dN}{dy}(b) = \frac{n(b)}{1 + \delta(A^{1/3} + B^{1/3})} \frac{dN_{pp}}{dy}, \quad (9)$$

where  $dN_{pp}/dy = 0.8 \ln \sqrt{s}$  is the hadron multiplicity for nucleon-nucleon collisions at mid-rapidity [31]. The value of  $dN/dy$  is 725 at  $b \sim 3.2$  fm,  $\sqrt{s} = 17.3$  GeV and  $\delta = 0.09$  (see Fig.1). The term  $1 + \delta(A^{1/3} + B^{1/3})$  takes into account the energy degradation of the participating nucleons in the nuclear environment. For isentropic expansion the initial temperature ( $T_i$ ) is related to the hadron multiplicity as,

$$T_i^3(b) = \frac{2\pi^4}{45\xi(3)} \frac{1}{\pi R_A^2 \tau_i 4a_k} \frac{dN}{dy}(b) \quad (10)$$

$a_k = \pi^2 g_k/90$  is determined by the statistical degeneracy ( $g_k$ ) of the system formed after the collisions. The statistical degeneracy of the hadronic phase composed of  $\pi$ ,  $\rho$ ,  $\omega$ ,  $\eta$ ,  $a_1$  and nucleons, is a temperature dependent quantity, its value is  $\sim 30$  near the critical temperature where the hadronic masses go to zero according to the universal scaling scenario [16]. The increase in the effective statistical degeneracy originates from the heavier hadrons going to massless ( see also [34]) situation. A value of  $g_{eff} \sim 30$  can also be realized from the lattice data [32,33] near the phase transition point by using the relation  $s/T^3 = 4\pi^2 g_{eff}/90$ , where  $s$  is the entropy density. For  $\tau_i = 1$  fm/c [35] and  $g_k \sim 30$ , we get an initial temperature  $T_i(b \sim 3.2$  fm)  $\sim 200$  MeV (see Fig. 1) in the ideal fluid approximation (please note that the variation of  $T_i(b)$  as a function of the impact parameter is

very slow because  $T_i(b) \sim [dN/dy(b)]^{1/3}$ . In an attempt to understand the lattice data in terms of the effective fields [36] the effective degrees of freedom in hadrons was limited to  $\sim 24$  which is the number of fundamental degrees of freedom for two quark flavors. In such a case the initial temperature will be slightly higher than 200 MeV. However, we recall here that the inclusion of the viscous effects in the system results in a smaller value of the initial temperature [37] depending on the value of the viscous coefficients ( $\eta$ ) on which useful constraints can be imposed as discussed in [38]. However, in the present calculation we will ignore any such effect.

The integration over the space time history has been performed by taking the temperature profile from the transport model [39] as well as by solving the (3+1)dimensional hydrodynamical equations. We discuss the results from transport model first, where the temperature varies with time as follows:

$$T(t) = (T_i - T_\infty)e^{-t/\tau} + T_\infty \quad (11)$$

The calculation is performed with two sets of parameters: (i)  $T_i = 170$  MeV,  $T_\infty = 110$  MeV,  $\tau = 8$  fm/c and (ii)  $T_i = 200$  MeV,  $T_\infty = 120$  MeV,  $\tau = 8$  fm/c. We observe (not shown in the figure) that thermal photon yield resulting from the first set of parameters underestimates WA98 spectra for both the scenarios I and II, probably indicating a higher initial temperature of the fire ball created after the nuclear collisions. Therefore, we will not discuss the case (i) further.

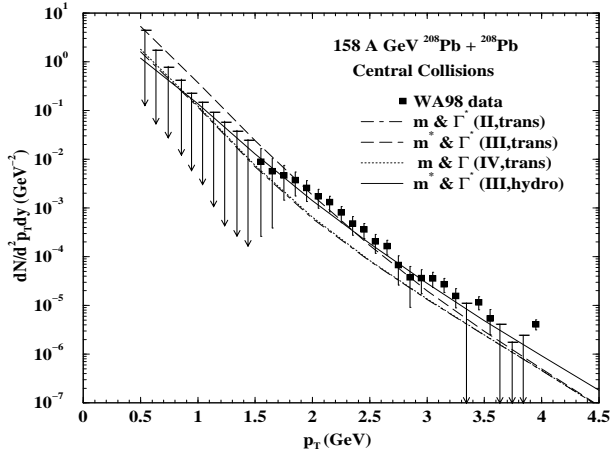


FIG. 4. Total (prompt+thermal) photon yield in Pb + Pb collisions at 158 A GeV at CERN-SPS. The theoretical calculations contain hard QCD and thermal photons. The system is formed in the hadronic phase with initial temperature  $T_i = 200$  MeV; ‘trans’ indicates the results for the cooling law 11.

In Fig. 4 the  $p_T$  distribution of photons (prompt+thermal) is compared with the WA98 data. Within the framework of the transport model (scenario (ii)) the data is well reproduced when the hadronic masses and decay widths are allowed to vary according

to the eqs. 5 and 6 respectively (long-dash line). Photon spectra for scenarios (I) and (III) give similar results and hence not shown separately. However, when scenario (II) is considered for thermal photons the experimentally observed “excess” photon in the region  $1.5 \leq p_T$  (GeV)  $\leq 2.5$  (dashed-dot line) is not reproduced. The dotted line indicates results with vacuum masses and widths.

Next we study the sensitivity of the results on the space-time evolution. In order to do that we solve the (3+1) dimensional hydrodynamic equations with initial energy density [40],

$$\epsilon(\tau_i, r) = \frac{\epsilon_0}{e^{(r-R_A)/\delta} + 1} \quad (12)$$

and initial velocity profile

$$v_r = v_0 \left( \frac{r}{R_A} \right)^\alpha \quad (13)$$

which has been successfully used to study transverse momentum spectra of hadrons [41,42] and photons [5,7]. For our numerical calculations we choose  $\alpha = 1$  and  $v_0 = 0$  at the initial time. The resulting photon yield for the scenario (I) is shown in Fig. 4 (solid line). With similar initial conditions the WA98 photon spectra is well reproduced in this case also.

The agreement between the results obtained with two different types of space time evolution scenarios (transport model and hydrodynamics) can be explained as follows. We find that the variation of temperature with time (cooling law) in eq. 11 is slower than the one obtained by solving hydrodynamic equations. As a consequence the thermal system has a longer life time than the former case, allowing the system to emit photons for a longer time. In case of hydrodynamics this is compensated by the transverse kick experienced by the photon at large  $p_T$  due to radial velocity of the expanding matter.

Now we study the invariant mass distribution of lepton pairs measured by CERES/NA45 collaboration in Pb + Au collisions. In Fig. 5 the experimental data is compared with the theoretical results for  $dN_{ch}/d\eta = 270$ . The observed enhancement of the dilepton yield around  $M \sim 0.3 - 0.6$  GeV can be reproduced by all the scenarios (I), (II) and (III) considered here. The data is also well reproduced when hydrodynamics is used to describe the space time evolution of the system for all the three scenarios considered here. However, with vacuum properties of the vector mesons the low mass enhancement can not be reproduced.

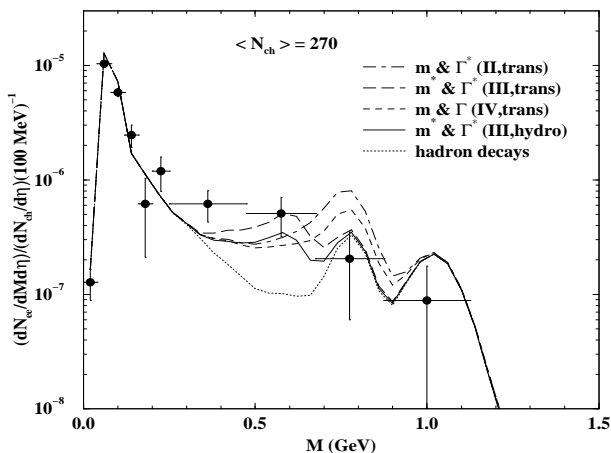


FIG. 5. Dilepton spectra for  $\langle N_{ch} \rangle = 270$  for different scenarios as indicated.

We conclude that the WA98 photon data can be described well with hadronic initial state at a temperature  $\sim 200$  MeV with masses of hadrons approaching to zero near the critical temperature. Similar value of the initial temperature is obtained in Refs. [6,7,43]. Based on the present and our earlier results [6], it is fair to say that a simple hadronic model is inadequate to explain the photon and dilepton data from WA98 and CERES collaborations respectively. Either a substantial change in the in-medium hadronic spectral function or the formation of the QGP is required to describe the data. The  $p_T$  distribution of photons is almost unaffected by the broadening of the vector meson spectral function in the medium. However, the invariant mass distribution of the lepton pairs can be explained by all the three scenarios, I, II and III. Thus by looking only at the dilepton spectra it is difficult to differentiate the above scenarios (situation may become better with the improvement of the experimental statistics). Therefore, a simultaneous measurement of photon and dilepton signals is not only important to study the formation of QGP [44] but it may also shed some light on the medium modification of the hadrons, which is known to be closely related to the restoration of chiral symmetry.

**Acknowledgement:** We are grateful to Tetsuo Hatsuda for useful comments on this manuscript. J.A. is grateful to the Japan Society for Promotion of Science (JSPS) for financial support. J.A. is also supported by Grant-in-aid for Scientific Research No. 98360 of JSPS.

---

[1] L. McLerran and T. Toimela, Phys. Rev. **D 31**, 545 (1985); C. Gale and J. I. Kapusta, Nucl. Phys. **B357**, 65 (1991); E. V. Shuryak, Phys. Rep. **61**, 71 (1980); J. Alam, S. Raha and B. Sinha, Phys. Rep. **273**, 243 (1996); W. Cassing and E. L. Bratkovskaya, Phys. Rep., **308**, 65

(1999).  
[2] M. M. Aggarwal et al., WA98 Collaboration, Phys. Rev. Lett. **85**, 3595 (2000).  
[3] S. Sarkar, P. Roy, J. Alam and B. Sinha, Phys. Rev. **C 60**, 054907 (1999).  
[4] C. Y. Wong and H. Wang, Phys. Rev. **C 58**, 376 (1998).  
[5] K. Gallmeister, B. Kämpfer and O. P. Pavlenko, Phys. Rev. **C 62**, 057901 (2000).  
[6] J. Alam, S. Sarkar, T. Hatsuda, T. K. Nayak and B. Sinha, Phys. Rev. **C 63**, 021901R (2001).  
[7] D. Yu. Peressounko and Yu. E. Pokrovsky, hep-ph/0009025.  
[8] D. K. Srivastava and B. Sinha, nucl-th/0006018.  
[9] C. Y. Wong, Introduction to high energy heavy ion collisions, World Scientific, Singapore, 1994.  
[10] K. J. Eskola, R. Vogt and X. N. Wang, Int. J. Mod. Phys. **A 10**, 3087 (1995).  
[11] J. F. Owens, Rev. Mod. Phys. **59**, 465 (1987).  
[12] H. L. Lai, et. al., Eur. Phys. J. **C 12**, 375 (2000).  
[13] E704 Collaboration, D. L. Adams et al, Phys. Lett. **B 345**, 569 (1995).  
[14] T. Ferbel and W. R. Molzon, Rev. Mod. Phys. **56**, 181 (1984).  
[15] P. Roy et. al. to be published.  
[16] G. E. Brown and M. Rho, Phys. Rep. **269**, 333 (1996); hep-ph/0103102.  
[17] T. Hatsuda and T. Kunihiro, Phys. Rep. **247**, 221 (1994).  
[18] R. D. Pisarski, hep-ph/9503330.  
[19] R. Rapp and J. Wambach, hep-ph/9909229 and references therein.  
[20] J. Alam, S. Sarkar, P. Roy, T. Hatsuda and B. Sinha, Ann. Phys.(NY), **286**, 159 (2000).  
[21] G. E. Brown and M. Rho, Phys. Rev. Lett. **66**, 2720(1991).  
[22] H. A. Weldon, Ann. Phys. (NY) **228**, 43 (1993).  
[23] J. I. Kapusta, P. Lichard, and D. Seibert, Phys. Rev. **D44**, 2774 (1991).  
[24] S. Sarkar, J. Alam, P. Roy, A. K. Dutt-Mazumder, B. Dutta-Roy and B. Sinha, Nucl. Phys. **A634**, 206 (1998); P. Roy, S. Sarkar, J. Alam and B. Sinha, Nucl. Phys. **A 653**, 277 (1999).  
[25] Baier, H. Nakkagawa, A. Niegawa and K. Redlich, Z. Phys. **C53**, 433 (1992).  
[26] P. Aurenche, F. Gelis, H. Zaraket and R. Kobes, Phys. Rev. **D 58**, 085003 (1998).  
[27] F. D. Steffen and M. H. Thoma, hep-ph/0103044.  
[28] D. Dutta, S. V. S. Sastry, A. K. Mohanty, K. Kumar and R. K. Choudhury, hep-ph/0104134.  
[29] D. K. Srivastava, B. Sinha, I. Kvasnikova and C. Gale, nucl-th/0101014.  
[30] F. Karsch, Z. Phys. **C38** 147 (1988).  
[31] U. Heinz, P. Koch and B. Friman, in Proc. Large Hadron Collider Workshop, Aachen, 1990, CERN-90-10, Vol. II, p. 1079.  
[32] F. Karsch, hep-ph/0103314.  
[33] M. Asakawa and T. Hatsuda, Phys. Rev. **D55**, 4488 (1997).  
[34] V. Koch and G. E. Brown, Nucl. Phys. **A 560**, 345 (1993).  
[35] J. D. Bjorken, Phys. Rev. **D27**, 140 (1983).

- [36] G. E. Brown, H. A. Bethe, A. D. Jackson and P. M. Pizzochero, Nucl. Phys. **A 560**, 1035 (1993).
- [37] S. Sarkar, P. Roy, J. Alam, S. Raha and B. Sinha, J. Phys. **G 23**, 469 (1997).
- [38] P. Danielewicz and M. Gyulassy, Phys. Rev. **D31**, 53 (1985).
- [39] G. Q. Li, C. M. Ko, G. E. Brown and H. Sorge, Nucl. Phys. **A 611**, 539 (1996).
- [40] H. von Gersdorff, M. Kataja, L. McLerran and P. V. Ruuskanen, Phys. Rev. **D 34**, 794 (1986).
- [41] P. Braun-Munzinger, J. Stachel, J. P. Wessels and N. Xu, Phys. Lett. **B 365**, 1 (1996).
- [42] U. Heinz, K. S. Lee and E. Schnedermann, in Quark Gluon Plasma, edited by R. C. Hwa, (World Scientific, Singapore 1992); J. Alam, J. Cleymans, K. Redlich and H. Satz, nucl-th/9707042.
- [43] R. Rapp E. Shuryak, Phys. Lett. **B 473**, 13 (2000); K. Gallmeister, B. Kämpfer and O. P. Pavlenko, Phys. Lett. **B 473**, 20 (2000); S. Sarkar, J. Alam and T. Hatsuda, nucl-th/0011032.
- [44] B. Sinha, Phys. Lett. **B 128** 91 (1983).